Microstructural Evolution of Iron-Oxide-Doped Alumina Nanoparticles Synthesized from Microemulsions

Pedro Tartaj*,† and Jesus Tartaj‡

Particulate Materials Department, Instituto de Ciencia de Materiales de Madrid (CSIC), Campus de Cantoblanco, 28049 Madrid, Spain and Electroceramic Department, Instituto de Cerámica y Vidrio (CSIC), 28500 Arganda del Rey (Madrid), Spain

Received March 14, 2001. Revised Manuscript Received November 30, 2001

A versatile and simple method for preparing highly homogeneous iron-oxide-doped alumina nanosized powders of different compositions is described. The method consists of the hydrolysis with ammonium hydroxide of aluminum and iron nitrate aqueous solutions confined within the reverse micelle nanocavities of water-in-oil microemulsions. The as-prepared powders were characterized in terms of phase composition, morphology, and chemical composition. The thermal evolution of these powders up to the formation of the thermodynamically stable α-Al_2O_3 phase was studied. Electron microscopy and density studies were also carried out to determine how the presence of iron oxide affects the microstructural development and sintering evolution of compact powders.

Introduction

Alumina is a material extensively used in the ceramic industry for structural and electrical applications.[1] Its properties in these areas are extremely dependent on the microstructure, which emphasizes the importance of designing new synthetic routes to achieve rigorous control of this parameter.

Considerable advances have been achieved in the field of ceramics by the development of new chemical processing routes that have allowed for the preparation of homogeneous and pure materials. However, these routes normally run to metastable phases that need to be thermally treated at high temperatures to obtain the thermodynamically stable phase. In the alumina system, the final transformation to the α phase (corundum) requires considerable thermal activation,[2] which is responsible for the grain coarsening of the compact powder. As a result, microstructures consisting of an extensive interconnected pore structure (known as vermicular) whose elimination requires temperatures of at least 1600 °C are developed.[3−6] The addition of seed particles that are structurally equivalent to the thermodynamically stable phase has been shown to be an adequate approach to preventing this type of microstructure.[3−6] Among the materials that can be used as seed sources, α-Fe_2O_3 (hematite) seems to accomplish the required conditions.[4−6] Hematite is isostructural with α-Al_2O_3, differing by only 5% in lattice parameter dimensions. Moreover, the presence of Fe_2O_3 can promote anisotropic grain growth.[7]

It is well-established that the incorporation of a second phase into a ceramic matrix can lead to significant increases in fracture toughness.[8] The ideal reinforcement material should have a thermal expansion coefficient similar to that of the matrix to avoid tensile stresses. Thus, the bimodal microstructure generated by the addition of Fe_2O_3 can lead to a new class of tough ceramic materials by allowing the in situ development of the self-reinforcing phase in the microstructure.[7,9,10]

Thus far, the most-employed method for preparing iron-oxide-doped alumina particles is based on a many-step colloidal sol−gel process,[4−6] which involves the use of a highly hydrolyzable precursor (aluminum *sec*-butoxide) and its further processing for about 1 week. In addition, as pointed out by McCardle and Messing,[4] this synthetic route is restricted (because of problems with the homogeneity) to an iron oxide initial content of about 4 wt %. Therefore, it seems appropriate to develop simple synthetic routes for the production of homogeneous iron-doped alumina nanosized powders with a broad range of compositions. This will allow for both the reduction of sintering temperatures and the promotion of controlled anisotropic grain growth.

Organized surfactant assemblies such as microemulsions, micelles, hexagonal phases, cubic phases, monolayers, and vesicles are unique reaction media that can solubilize, concentrate, localize, and even organize the reactants.[11] In particular, water-in-oil (W/O) micro-

* Address for correspondence: Pedro Tartaj, Instituto de Ciencia de Materiales de Madrid (CSIC), Campus de Cantoblanco, 28049 Madrid, Spain. Fax: 34-913720623. E-mail: ptartaj@icmm.csic.es.
† Instituto de Ciencia de Materiales de Madrid.
‡ Instituto de Cerámica y Vidrio.

(1) Dorre, E.; Hubner, H. *Alumina: Material Research and Engineering*; Springer-Verlag: New York, 1984.
(2) Dynys, F. W.; Halloran, J. W. *J. Am. Ceram. Soc.* **1982**, *65*, 442.
(3) Shelleman, R. A.; Messing, G. L.; Kumagai, M. *J. Non-Cryst. Solids* **1986**, *82*, 277.
(4) McArdle, J. L.; Messing, G. L. *Adv. Ceram. Mater.* **1988**, *3*, 387.
(5) McArdle, J. L.; Messing, G. L. *J. Am. Ceram. Soc.* **1993**, *76*, 214.
(6) Tartaj, J.; Messing, G. L. *J. Mater. Sci. Lett.* **1997**, *16*, 168.
(7) Tartaj, J.; Messing, G. L. *J. Eur. Ceram. Soc.* **1997**, *17*, 719.
(8) Farkash, M. J.; Brandon, D. *Mater. Sci. Eng. A* **1994**, *177*, 269.
(9) Rödel, J.; Glaeser, A. M. *J. Am. Ceram. Soc.* **1994**, *73*, 3292.
(10) Carisey, T.; Levin, I.; Brandon, D. G. *J. Eur. Ceram. Soc.* **1995**, *15*, 283.
(11) Fendler, J. H. *Membrane Mimetic Chemistry: Characterization and Applications of Micelles, Microemulsion, Monolayers, Bilayers, Vesicles, Host−Guest Systems and Polyions*; Wiley: New York, 1975.

10.1021/cm011085l CCC: $22.00
Published on Web 01/24/2002

emulsions (i.e., reverse micelles) are a simple method for preparing homogeneous nanosized powders.[12−15] In these systems, the surfactant-stabilized microcavities (∼10 nm) provide a confinement effect that limits particle nucleation, growth, and agglomeration.[16] Therefore, the possible compositional homogeneity at the nanoscale level (i.e., decrease in diffusion distances) achieved by this method is expected to enhance the effect of the Fe_2O_3 seed particles on lowering the temperature required for α-Al_2O_3 formation.

This paper reports a versatile and simple method for preparing highly homogeneous iron-oxide-doped alumina nanopowders of different compositions using a microemulsion-mediated process. The powders thus obtained have been characterized in terms of phase composition, morphology, and chemical composition. We have also studied the thermal evolution up to corundum formation to relate the microstructure of the sintered powder to the iron oxide content.

Experimental Section

Chemicals. Water-in-oil microemulsions (reverse micelles) were prepared using Igepal Co520 (Aldrich) as the surfactant. Cyclohexane (Aldrich, 99.5% anhydrous) dehydrated with molecular sieves was used as the continuous oil phase. $Al(NO_3)_3 \cdot 9H_2O$ (Aldrich, 99%), $Fe(NO_3)_3 \cdot 9H_2O$ (Aldrich, 99%), ammonium hydroxide (Aldrich, 29%), and ethanol (Aldrich, 99.5% anhydrous) were used as received. Deionized water was used in all experiments.

Synthesis. The microemulsions were prepared at room temperature by the addition of 2.5 M aqueous solutions containing the aluminum and iron salts to a solution containing the surfactant and cyclohexane. The amount of surfactant was systematically varied to produce stable microemulsions containing the highest possible salt concentration. It was found that, for a surfactant concentration of 0.4 M, a maximum value of 0.4 M in salt concentration could be used. Higher salt concentrations, irrespective of the amount of surfactant added, failed to produce stable microemulsions. Therefore, the surfactant and salt concentrations were fixed at a value of 0.4 M. Under these particular conditions, five different samples containing different amounts of iron oxide (AF0, AF2, AF4, AF8, and AF16) were prepared. The weight ratio expressed as $Fe_2O_3/(Fe_2O_3 + Al_2O_3)$ was 0, 2, 4, 8, and 16% for samples AF0, AF2, AF4, AF8, and AF16, respectively. Alumina powders with higher iron contents were not studied because, as described in the Results and Discussion section, high values are expected to be detrimental to well-developed microstructures. To obtain microemulsions, the solutions were thoroughly shaken for 5 min and then stirred for 1 h. After that, the solutions became transparent, and no turbidity developed with time, which indicated the formation of stable microemulsions.

The controlled hydrolysis of the aluminum and iron nitrate salts was carried out by adding to the microemulsion an equal volume of a 4 M ammonium aqueous solution. The mixture thus generated was kept under magnetic stirring for 2 h. Then, a 10% volume of EtOH was added to the system to destabilize the suspension and facilitate the centrifugation process. Finally, the powder was washed several times with $EtOH/H_2O$ and dried at 50 °C overnight.

Characterization Techniques. The different phases present in the solids were assessed by X-ray diffraction (XRD, PW1710, Philips) and infrared (IR) spectroscopy (20SXC, Nicolet). To record the infrared spectra, the powders were diluted in a KBr matrix. Cell parameters were determined by a least-squares fit of the XRD data using silicon as the reference standard. Thermogravimetric (TGA) and differential thermal (DTA) analyses (Netsch STA 781, Stanton) were conducted in dynamic air at a heating rate of 10 °C min^{-1}.

The morphology of the powders was examined by transmission electron microscopy (TEM, 2000 FX2, JEOL). Chemical analyses of the samples were carried out by plasma emission analysis (ICP, 5500, Perkin-Elmer). Chemical analyses of selected areas of about 25 nm were carried out with an energy-dispersive spectrometry analyzer (QX 2000, Oxford Link) integrated into the TEM.

For densification studies, the precursors were ground with a mortar and heated to the temperature of complete corundum formation. Then, calcined powders were attrition milled with alumina balls for 1 h in 2-propanol (Aldrich, 99%) and dried at 80 °C overnight. After that, the powders were isopressed at 200 MPa and again heated at different temperatures to follow the evolution of sintering. The density of the sintered bodies was measured by the Archimedes method using distilled water. Microstructure development was observed by scanning electron microscopy (SEM, DSM 960, Zeiss) on polished and thermally etched surfaces.

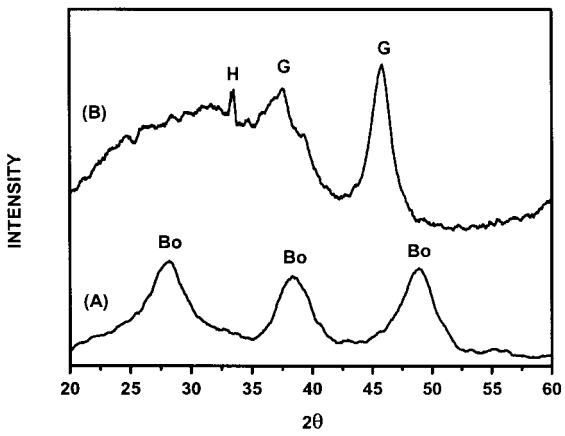

Figure 1. (A) XRD pattern representative of the powder generated after the hydrolysis of aluminum and iron nitrate salts with NH_4OH. (B) XRD pattern of sample AF16 heated at 500 °C. The symbols stand for Bo (boehmite), G (γ-Al_2O_3), and H (α-Fe_2O_3).

Results and Discussion

Sample Characterization. The powders obtained from the microemulsions displayed diffraction peaks associated with only boehmite,[17] irrespective of the iron content. An XRD pattern representative of all samples is shown in Figure 1. The chemical composition of the powders was equal to that of the starting liquid mixtures, which indicated perfect control of the stoichiometry. A TEM micrograph also representative of all samples is shown in Figure 2. As observed, the powders consist of soft aggregates composed of nanoparticles of about 10 nm. TEM microanalysis carried out on selected areas of about 25 nm showed a chemical composition similar to the average composition of powders determined by ICP. Therefore, the high degree of mixing of the powders indicates the presence of iron oxide seeds of a size smaller than 25 nm. This is expected to maximize the induced nucleation rate and to limit (if benefit) the addition of iron oxide (i.e., for a fixed amount of seeds, as their size decreases, more sites are available for heterogeneous nucleation).[4] Also, it is

(12) Lisiecki, I.; Pileni, M. P. *J. Am. Chem. Soc.* **1993**, *115*, 7.
(13) Zhang, K.; Chew, C. H.; Xu, G. Q.; Wang, J.; Gan, L. M. *Langmuir* **1999**, *15*, 3056.
(14) Zarur, A. J.; Ying, J. Y. *Nature* **2000**, *403*, 65.
(15) Liu, C.; Zhang, A. J. *Chem. Mater.* **2001**, *13*, 2092.
(16) Pileni, M. P. *J. Phys. Chem.* **1993**, *97*, 6961.
(17) JCPDS file 21-1307.

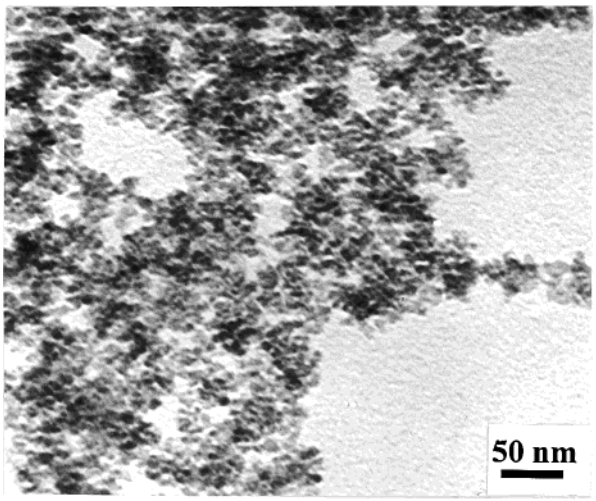

Figure 2. TEM micrograph of the powder generated after the hydrolysis of aluminum and iron nitrate salts with NH_4OH.

worth mentioning the high compositional homogeneity of the powders with initial iron oxide contents of 16 wt %, unlike that observed in samples prepared by the colloidal sol−gel method.[4]

Cell parameter measurements were carried out in boehmite samples to investigate the possible presence of iron cations within the boehmite structure, but because of the lack of crystallinity, i.e., very broad diffraction peaks, the high standard deviation values obtained precluded us from having statistically reliable results.

IR spectroscopy has been shown to be a very sensitive technique for detecting the possible substitution of Al^{3+} by Fe^{3+} cations or vice versa.[18−20] However, caution should be taken when interpreting the IR absorption spectra of powders, especially those of polar solids. Even though the IR absorption spectrum of a powder is mainly determined by its chemical composition and structure, in the case of polar solids, is strongly influenced by the crystal shape an aggregation state of the particles.[21] This is due to the polarization effects induced on the particle surface by the electromagnetic field of the incident radiation, which can give rise to important variations in the position, relative intensity, and width of the bands.[22] For boehmite-type structures, as the crystals change from plates to rods, the vibrations in the [010] direction decrease in frequency, whereas those parallel to the [001] direction are unaffected.[20] The in-(100)-plane bending bond that lies at 1070 cm^{-1} is parallel to the [001] direction, and therefore, the possible changes in the position of this band must be associated only with changes in the chemical composition of the boehmite structure. In particular, one should expect a shift of this vibrational mode to lower frequencies as the Fe^{3+} content within the boehmite structure increases.[20]

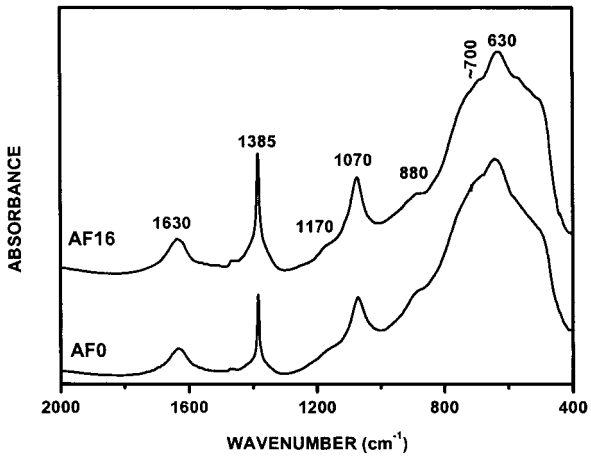

Figure 3. IR spectra of samples AF0 and AF16 generated after hydrolysis with NH_4OH.

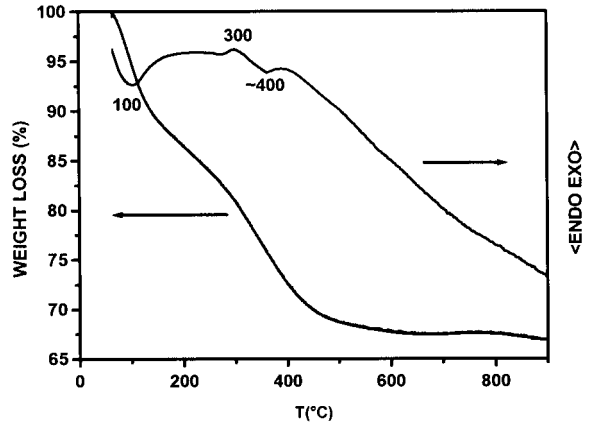

Figure 4. DTA/TGA curves of a representative powder sample (AF4).

The IR spectra of the samples with zero (AF0) and the maximum (AF16) iron content are displayed in Figure 3. No changes in the position of the band that lies at 1070 cm^{-1} are detected, which suggests that Fe^{3+} is not located within the boehmite structure and, therefore, that it is most likely in the form of an hydroxide. In principle, both the low amount of this iron hydroxide and its lack of crystallinity would prevent this phase from being detected by IR spectroscopy. In addition to the band at 1070 cm^{-1}, the spectra display bands at 1170, 880, 700, and 630 cm^{-1}, which are associated also with boehmite.[23] Other bands at 3420 (region of the spectrum not shown) and 1630 cm^{-1} due to the stretching and deformation vibration modes of free water were also detected. Finally, the spectra displayed a band at 1385 cm^{-1} assigned to residual nitrate species that were not leached out during the washing procedure.

Thermal Evolution of Powders. The DTA and TGA curves of sample AF4 (chosen as representative of all samples) recorded up to a temperature of 900 °C are displayed in Figure 4. DTA analyses show an endothermic effect at about 100 °C associated with the release of adsorbed water and alcohols. An exothermic peak at about 300 °C was assigned to the elimination of residual nitrate species coming from the iron and

(18) Tarte, P. *Spectrochim. Acta* **1967**, *23A*, 2127.
(19) Prieto, M. C.; Gallardo-Amores, J. M.; Sánchez-Escribano, V.; Busca, G. *J. Mater. Chem.* **1994**, *4*, 1123.
(20) Cornell, R. M.; Schwertmann, U. *The Iron Oxides. Structure, Properties, Reactions, Occurrence and Uses*; VCH: Weinheim, Germany, 1996.
(21) Serna, C. J.; Rendón, J. L.; Iglesias, J. E. *Spectrochim. Acta* **1982**, *38A*, 797.
(22) Ruppin, R.; Englman, R. *Rep. Prog. Phys.* **1970**, *33*, 149.
(23) Stegmann, M. C.; Vivien, D.; Mazieres, C. *Spectrochim. Acta* **1972**, *29A*, 1653.

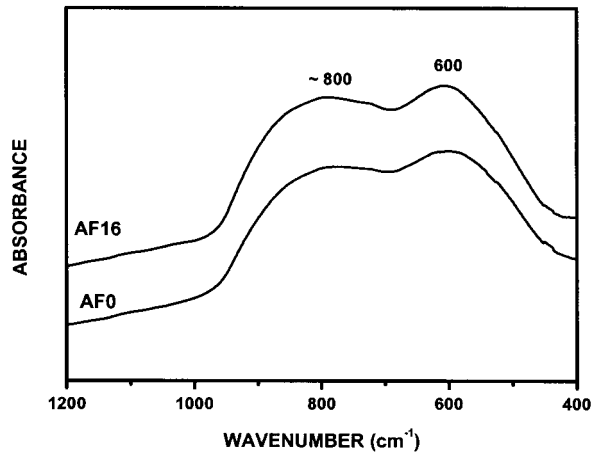

Figure 5. IR spectra of samples AF0 and AF16 heated at 500 °C.

aluminum precursors. In accordance with this result, at this temperature, the vibration mode at 1385 cm^{-1} associated with nitrate species was not detected by IR spectroscopy (data not shown). The topotactic decomposition of boehmite to form the anhydrous defect spinel structure (γ-Al_2O_3) was detected by the presence of an endothermic peak centered at about 400 °C. The presence in the IR spectra of the samples heated at 500 °C of bands at 800 and 600 cm^{-1} (Figure 5), also due to the spinel phase,[24,25] confirmed the results obtained by DTA. The observed very broad bands suggest a random distribution of cations and vacancies in the γ-Al_2O_3 structure. It is important to stress that the IR spectra of all samples heated at this temperature showed no differences in the position of the bands. This result suggests that, at this point, the Fe^{3+} cations had not yet diffused into the spinel phase and, therefore, that they were present as a separate oxide phase (most likely α-Fe_2O_3). In fact, the XRD pattern of the sample with the highest iron content (AF16) indicated the presence of α-Fe_2O_3 in addition to the γ-Al_2O_3 phase (Figure 1). With increasing temperature up to 900 °C, no features were observed in the DTA results, even though both XRD and IR spectroscopy indicated the transformation of γ- to δ- and θ-Al_2O_3 (data not shown). This is not surprising as transitions to the δ- and θ-Al_2O_3 phases involve only a continuous ordering of the vacant sites.[19,26−27] Finally, the weight loss associated with all of these processes (elimination of adsorbed water, alcohols, and residual nitrate species and dehydroxylation of boehmite) measured by TGA (Figure 4) was about 35%.

The transition from θ- to α-Al_2O_3 is detected in the DTA curve because it requires a reconstructive transformation, in which a restacking of the close-packed oxygen ion layer along with the simultaneous movement of metal ions must take place.[2] The DTA transition temperatures of all samples are shown in Table 1. For a heating rate of 10 °C min^{-1}, the transformation (as confirmed by XRD) appears at 1208 °C for the sample with no iron content (AF0). As the iron content increases, the transformation is detected at lower temperatures (Table 1), being decreased to 935 °C for the case of the sample with the highest iron content (AF16) (Table 1). The presence of iron oxide introduces preferred nucleation sites, thus reducing the activation barrier for nucleation and favoring the formation of stable α-Al_2O_3 nuclei.[4−6] As expected, the complete transformation to α-Al_2O_3 was different for all samples. In particular, in samples AF16 and AF8, this transformation was completed after heating at 900 and 950 °C, respectively, for 2 h. Meanwhile, in samples AF4 and AF2, the transformation was completed at 1000 °C, and in sample AF0, at 1200 °C, also after heating for 2 h.

Table 1. Effect of Fe_2O_3 on the θ- to α-Al_2O_3 Transformation Temperature

	AF0	AF2	AF4	AF8	AF16
DTA transformation temperature (°C)	1208	995	974	959	935

To obtain additional information on the presence of iron within the corundum structure, cell parameters of all samples heated at 1200 °C for 2 h were estimated (Table 2). Expansion of the unit cell was observed as the iron content increased, providing evidence of the substitution of Al^{3+} by Fe^{3+} cations. The linear expansion of the *c* parameter (Figure 6) as a function of the mole fraction of the solute, i.e., Vegard's law,[28] indicated that all of the Fe^{3+} cations were randomly distributed within the corundum structure, even in the sample with a 10.8% mole fraction of the solute (AF16). In accordance with this result, the peak corresponding to α-Fe_2O_3 detected by XRD at 500 °C was not detected in sample AF16. On increasing the temperature to 1400 °C, the cell parameters of the samples with an Fe_2O_3 content of less than or equal to 8 wt % did not present changes with respect to those of the samples heated at 1200 °C (Table 2). However, in the sample with the highest iron content (AF16), a contraction of the cell parameters was detected (Table 2). At 1400 °C, reduction of some of the Fe^{3+} cations to give Fe^{2+} cations is thermodynamically favored.[29] Provided that the solubility of Fe^{2+} in the corundum structure is reported to be about 2 wt %,[30] much lower than that of Fe^{3+} cations (∼16 wt %),[30] the detected contraction of the cell parameters could be linked to the "exsolution" at high temperatures of the Fe^{2+} cations in the sample with the highest iron content. In all other samples, the amount of Fe^{2+} present in the system is below the solubility limit in the corundum structure, and therefore, no exsolution at high temperatures occurs. By supposing that Vegard's law applies for the iron cations forming a solid solution within the corundum structure (which, as mentioned above, seems to be a good supposition), we can estimate that the amount of free iron oxide (i.e., not forming a solid solution within the corundum structure) in sample AF16 after heating at 1400 °C is about a 2 wt %.

Segregation of Fe^{2+} cations to high-energy nonbasal grain boundaries enhances the grain boundary diffusivity, resulting in rapid growth and uncontrolled

(24) Ishii, M.; Nakahira, M.; Yamanaka, T. *Solid State Commun.* **1972**, *11*, 209.
(25) Baraton, M. I.; Quintard, P. *J. Mol. Struct.* **1982**, *79*, 337.
(26) Wilson, S. J.; Mcconnell, J. D. C. *J. Solid State Chem.* **1980**, *34*, 315.
(27) Busca, G.; Lorenzelli, G.; Guidetti, G.; Sánchez-Escribano, V. *Chem. Mater.* **1992**, *4*, 595.
(28) West, A. R. *Solid State Chemistry and its Applications*; Wiley: New York, 1984.
(29) Muan, A.; Phillips, B. *J. Phys. Chem.* **1960**, *64*, 1451.
(30) Muan, A. *Am. J. Sci.* **1958**, *256*, 413.

Table 2. Values of the *c* Parameter (nm) at 1200 and 1400 °C for All Samples

T (°C)	AF0	AF2	AF4	AF8	AF16	hematite[a]
1200	1.2992 (2)	1.3004 (2)	1.3011 (3)	1.3033 (3)	1.3075 (2)	1.3749 (1)
1400	1.2993 (2)	1.3004 (2)	1.3012 (2)	1.3033 (3)	1.3063 (2)	1.3749 (1)

[a] Data for hematite were taken from JCPDS file 33-664.

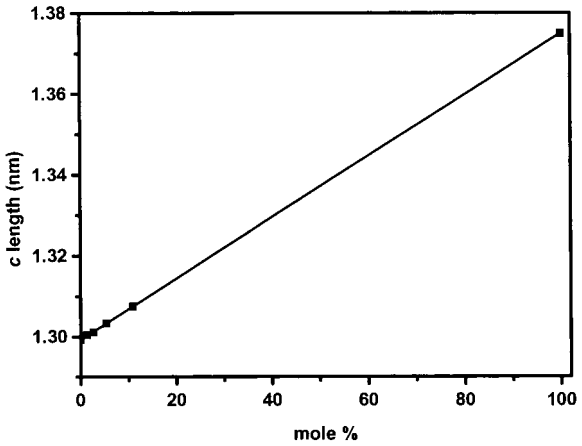

Figure 6. Evolution of the *c* parameter as a function of the iron content (■) and best least-squares linear fit (—).

microstructural development.[31] Therefore, even though sample AF16 presents the lower temperature of complete corundum formation (900 °C), the presence of free iron precludes us from using this sample to prepare compact powders. This result turned out to be the reason for which samples with iron oxide contents higher than 16 wt % were not studied.

Bulk Microstructure Development and Sintering Behavior. For transition aluminas, it has been suggested that the microstructural evolution is essentially controlled by the θ-to-α transformation.[2,32−33] Special mention is merited by the work of Wu and De Jonghe[33] on γ-Al_2O_3 nanophase powders prepared by the gas condensation technique, in which they indicate the benefits of heating the loose powder, prior to compaction, to develop the α phase. As concluded above, formation of the α phase starting from precursors obtained from microemulsions also involves a series of transition aluminas. Therefore, following Wu and De Jonghe,[33] the microstructural development was monitored by SEM for samples previously heated to the temperature of α-Al_2O_3 formation.

Three samples were selected for this study, the unseeded sample (AF0) and those with 4 (AF4) and 8 (AF8) wt % iron contents. The transformation to the α phase of the loose powder was carried out by heating the unseeded sample for 2 h to 1200 °C and the seeded samples also for 2 h but to 1000 (AF4) and 950 °C (AF8). The heating rate was equal to 20 °C min^{-1} in both cases.

The microstructures of α-Al_2O_3 compact powders with different iron contents heated at 1400 °C are displayed in Figure 7. This temperature was selected because the effect of iron content on microstructure is clearly noticed. The unseeded sintered sample heated at this temperature (Figure 7a) shows the characteristic vermicular grain structure of α-Al_2O_3, retaining a high fraction of porosity (85% of the theoretical density). In contrast, the sample with the 4 wt % iron oxide content develops a dense microstructure (99% of the theoretical density) with a uniform grain structure of equiaxed and

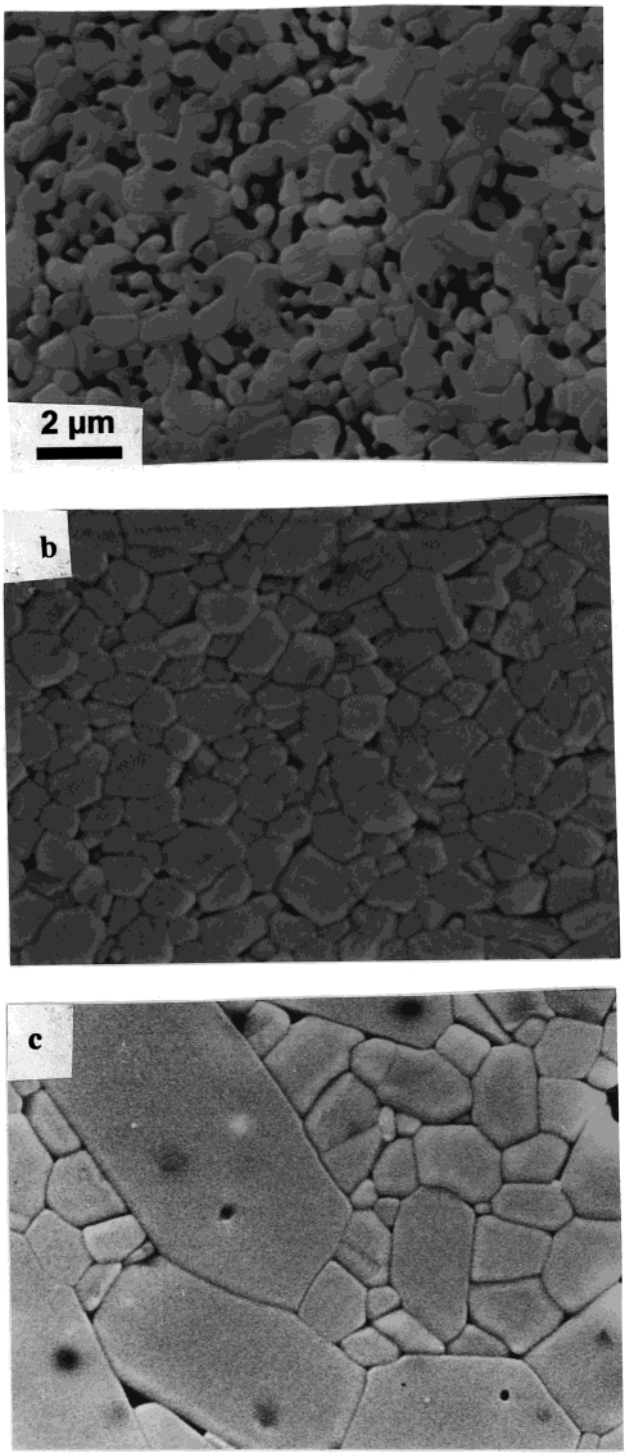

Figure 7. SEM images of samples (a) AF0, (b) AF4, and (c) AF8 first heated to the temperature of corundum formation; then isopressed at 200 MPa; and finally, heated at 1400 °C for 2 h. The scale bar corresponds to all images shown.

(31) Ikuma, Y.; Gordon, R. S. *J. Am. Ceram. Soc.* **1983**, *66*, 139.
(32) Badkar, P. A.; Bailey, J. E. *J. Mater. Sci.* **1976**, *11*, 1794.
(33) Wu, S. J.; Rahaman, M. N.; De Jonghe, L. C. *J. Am. Ceram. Soc.* **1996**, *79*, 2207.

faceted grains (Figure 7b). Sample AF8 also reached nearly theoretical density (99%) at this temperature, but as is shown in Figure 7c, the sample developed a bimodal microstructure with large grains in a matrix consisting of finer grains. Anisotropic grain growth in iron-oxide-doped Al_2O_3 powder compacts could be attributed to the presence of Fe^{2+} cations forming a solid solution within the corundum structure.[7] The reduction of Fe^{3+} to give Fe^{2+} cations at high temperatures produces oxygen vacancies to maintain electrical neutrality of the corundum crystal, and therefore, the diffusive mass transport is likely to be enhanced. The pores inside the grains, which one can speculate are associated with gas evolution as result of O_2 release, support this evidence. The above-mentioned exsolution of iron from the corundum structure detected in sample AF16 by measuring cell parameters would support the presence of Fe^{2+} cations at high temperature.

Conclusions

It has been shown that highly homogeneous nanostructured iron-doped alumina powders can be prepared by the hydrolysis of iron and aluminum nitrate aqueous solutions confined within the nanodroplets of water-in-oil microemulsions. The method, when compared with the traditional colloidal sol−gel process, largely simplifies the production of boehmite powders and allows for the preparation of homogeneous powders containing larger amounts of iron. In addition, by the adequate selection of the surfactants (Igepal Co520) and the organic solvent (cyclohexane), microemulsions containing high element concentrations were prepared. It has been determined that the iron content had a pronounced effect on the temperature of α-Al_2O_3 formation as well as on the microstructure development and the sintering evolution of the compact powders. In particular, nearly theoretical density was detected only in iron-doped α-Al_2O_3 samples heated at temperatures of about 1400 °C. Finally, the anisotropic grain growth observed only for the iron-doped α-Al_2O_3 samples was associated with the presence at high temperatures of Fe^{2+} cations.

CM011085L